

A fast radiative transfer model for assimilation of satellite radiance observations - RTTOV-5

R. Saunders, M. Matricardi and P. Brunel

Research Department

May 1999

This paper has not been published and should be regarded as an Internal Report from ECMWF.
Permission to quote from it should be obtained from the ECMWF.





ABSTRACT

To assimilate atmospheric and surface radiance measurements from satellites in a numerical weather prediction (NWP) model a fast radiative transfer model is required, to compute radiances from the model first guess fields at every observation point. Such a model for satellite infrared and microwave radiance measurements is used for the assimilation of Advanced TIROS Operational Vertical Sounder (ATOVS) radiances, Meteosat clear sky radiances and Special Sensor Microwave Imager radiances at ECMWF. The model has been developed to include temperature, water vapour and ozone in the input profile and has been generalised to compute radiances for many different satellite radiometers using the same code. It is demonstrated, by comparisons with accurate line-by-line model computed radiances, that the fast model can reproduce the line-by-line model radiances for the ATOVS upper tropospheric and stratospheric temperature sounding channels to an accuracy below the instrumental noise. The lower tropospheric, surface sensing, water vapour and ozone channel radiances are not as well predicted but still accurately enough for NWP assimilation purposes. A comparison of measured ATOVS radiances with predicted values from NWP model analyses shows larger differences than would be predicted for most channels from only the combination of the fast radiative transfer model and instrument related errors.

1. INTRODUCTION

The use of the data from the TIROS Operational Vertical Sounder, TOVS, on the NOAA polar orbiting satellites (see *Smith et al.*, 1979 for more details) for global numerical weather prediction (NWP) in recent years has been changing from assimilating retrieved temperature and moisture profiles to direct assimilation of the measured radiances. The radiance increments (differences between the model first guess and measured values) can be used to influence the model temperature, water vapour and optionally ozone fields to obtain an optimal fit between all the observations assimilated and the model first guess (typically a 6 hour forecast). This direct use of the radiances has been operational at the European Centre for Medium Range Weather Forecasts (ECMWF) in one form or other since 1992 (see *Saunders et al.*, 1997, 1999a for more details of the use of TOVS data over the past few years). This approach has led to significant improvements in the quality of the NWP analyses and forecasts (*Eyre et al.*, 1993, *Andersson et al.*, 1994, *Derber and Wu*, 1998, *Kelly*, 1997, *Andersson et al.* 1998) particularly in the southern hemisphere and tropics.

To enable the assimilation of satellite sounder or imager radiances in a variational assimilation scheme (for example 1D-Var described by *Eyre et al.* (1993) for a single profile retrieval or 4D-Var described by *Rabier et al.* (1998) for a global NWP analysis) it is necessary to compute a first guess radiance from the model fields corresponding to every measured radiance. All observation types assimilated in the analysis have an "observation operator" in one form or another as described by *Andersson et al.* (1998). For satellite radiances this operator includes interpolating the model fields to the observation location and time and on to fixed pressure levels for the radiative transfer computation. The interpolated/extrapolated model profile and surface parameters are input to a fast radiative transfer model, the key part of the operator, to compute radiances for the required radiometer channels. This computation is commonly referred to as the "forward model". In the process of data assimilation the differences between the measured and first guess radiances are then used along with all the other observation differences to perturb the first guess fields to minimize the fit of the analysis to all the observations and the first guess fields taking into account their respective errors. In variational analyses this is achieved using the Jacobians (partial derivatives) of the radiative transfer model which allows the gradient of each of the atmospheric/surface variables with respect to the radiances and other observations to be computed for the first guess profile (*Thépaut*



and Moll, 1990). The radiative transfer model and its tangent-linear/adjoint are therefore a key component to enable the assimilation of radiance measurements in a NWP assimilation system.

The first version of the fast radiative transfer model (RTTOV-3) described by Eyre (1991) and Rizzi and Matricardi (1998) was used operationally at ECMWF from 1992 to 1998 and included temperature profiles from the surface to 0.1 hPa (extrapolated from the model profile above 10hPa), water vapour profiles from the surface to 300 hPa and surface temperature, humidity and pressure in the input profile. It has also been used at several other NWP centres (e.g. Derber and Wu, 1998). The new model (RTTOV-5) described here extends the water vapour profile to 0.1hPa and allows ozone sensitive channels to be simulated by including ozone as an additional input profile variable. It also allows surface emissivity to be input for each channel and for the microwave channels over sea the emissivities can be optionally computed internally from the input surface wind speed and temperature.

Radiances for several satellite instruments have been simulated using this model, in addition to the TOVS and Advanced TOVS (ATOVS) radiances, the Special Sensor Microwave Imager radiances on the U.S. Defense Meteorological Program Satellites, METEOSAT water vapour channel radiances (Kelly *et al.* 1996) and Vertical Temperature Profiler Radiometer infrared radiances (the predecessor to the TOVS instruments).

This paper documents results from this new version of the fast radiative transfer model RTTOV-5. The fast model RTTOV-3 was originally based on the work of McMillin *et al.* (1979) and Eyre and Woolf (1988) to which the interested reader is referred to for more details of the underlying theory of fast transmittance models. Rizzi and Matricardi (1998) have recently documented the performance of RTTOV-3 by comparing it with measured TOVS radiances and discussed the possible reasons for the radiance differences observed. They also describe an upgrade to RTTOV-3 where the TOVS transmittances were recomputed using the HARTCODE line by line model (Miskolczi *et al.*, 1988) in place of the old *tranh* transmittances (Weinreb *et al.*, 1981) used previously as the dependent set for RTTOV-3.

The performance of RTTOV-5 is described in this report for the High resolution Infrared Sounder (HIRS), Microwave Sounding Unit (MSU) and Advanced Microwave Sounding Unit (AMSU) simulated radiances in terms of ability to reproduce accurate line-by-line model transmittances and radiances for both dependent and independent sets of computed values. Measured TOVS and AMSU radiances are also compared with simulations using RTTOV-5, with NWP model fields providing the first guess profile vector, and the differences compared with those obtained from the line-by-line model comparisons. Complimentary results comparing the old (RTTOV-3) and new (RTTOV-5) model are described in Saunders *et al.* (1999b). In addition the Jacobians of the model showing where the radiances are sensitive to changes in the profile vector are also documented there. More technical details of the RTTOV-5 model, which provides guidance for users of the code, are given in Annex A of this report.

2. THE FORMULATION OF THE RADIATIVE TRANSFER MODEL

The formulation of the model is given in *Eyre (1991)* and *Eyre and Woolf (1988)*. For completeness the main components of the model are also described here.

2.1. Radiative transfer

The model uses an approximate form of the atmospheric radiative transfer (RT) equation. The top of the atmosphere upwelling radiance, $L(\nu, \theta)$, at a frequency ν and viewing angle θ from zenith at the surface, neglecting scattering effects, can be written as:

$$L(\nu, \theta) = (1 - N)L^{Clr}(\nu, \theta) + NL^{Cld}(\nu, \theta) \quad (1)$$

where $L^{Clr}(\nu, \theta)$ and $L^{Cld}(\nu, \theta)$ are the clear sky and fully cloudy top of atmosphere upwelling radiances and N is the fractional cloud cover. $L^{Clr}(\nu, \theta)$ can be written as:

$$L^{Clr}(\nu, \theta) = \tau_s(\nu, \theta)\epsilon_s(\nu, \theta)B(\nu, T_s) + \int_{\tau_s}^1 B(\nu, T)d\tau + (1 - \epsilon_s(\nu, \theta))\tau_s^2(\nu, \theta) \int_{\tau_s}^1 \frac{B(\nu, T)}{\tau^2} d\tau \quad (2)$$

where the first and third terms on the RHS of equation 2 are the radiance from the surface (emitted and reflected assuming specular reflection) and the second term is the radiance emitted by the atmosphere where $B(\nu, T)$ is the Planck radiance for a scene temperature T , $\tau_s(\nu, \theta)$ is the surface to space transmittance, τ the layer to space transmittance, $\epsilon_s(\nu, \theta)$ the surface emissivity, T is the layer mean temperature and T_s , the surface radiative temperature. $L^{Cld}(\nu, \theta)$ is defined as:

$$L^{Cld}(\nu, \theta) = \tau_{Cld}(\nu, \theta)B(\nu, T_{Cld}) + \int_{\tau_{Cld}}^1 B(\nu, T)d\tau \quad (3)$$

where $\tau_{Cld}(\nu, \theta)$ is the cloud top to space transmittance and T_{Cld} the cloud top temperature, the emissivity of the cloud top is assumed to be unity which is a tolerable assumption for optically thick water cloud at infrared radiances but not valid for optically thin cloud and all cloud at microwave frequencies. The latter will require a different treatment similar to a variable gas profile.

Making the same assumption as *McMillin et al. (1979)* that equations 2 and 3 still apply when integrated over the spectral response of a satellite radiometer channel, i , and rewriting in discrete layer notation for J atmospheric layers (level $j=1$ to J_s from the top to the layer above the surface) and for a single viewing angle just to simplify the notation we get:

$$L_i^{Clr} = \tau_{i,s}\epsilon_{i,s}B_i(T_s) + \sum_{j=1}^{J_s} L_{i,j}^u + (1 - \epsilon_{i,s}) \sum_{j=1}^{J_s} L_{i,j}^s \left[\frac{\tau_{i,s}^2}{(\tau_{i,j-1}\tau_{i,j})} \right] + L_i' \quad (4)$$

where L_i^{Clr} is the clear radiance and $\tau_{i,j}$ is the transmittance from level j to space integrated over the channel i spectral response. L_i' is a small atmospheric contribution from the surface to the first layer above the surface J_s . $L_{i,j}^u$ is defined as:

$$L_{i,j}^u = \frac{1}{2} [B_i(T_j) + B_i(T_{j-1})] (\tau_{i,j-1} - \tau_{i,j}) \quad (5)$$

The modified Planck function $B_i(T)$ takes account of the averaging of the true Planck function over the spectral response of channel i for scene temperature T and is given by,

$$B_i(T) = \frac{c_{1,i}}{[\exp(c_{2,i}/(a_i + b_i T)) - 1]} \quad (6)$$

where $c_{1,i} = c_1 v_i$ and $c_{2,i} = c_2 v_i$ with c_1 and c_2 the Planck function constants and v_i the central frequency of the channel i . a_i and b_i are the so-called “band correction coefficients” (see *Weinreb et al.*, 1981; *Lauritson et al.*, 1979), and are computed from the channel filter response.

Equation 5 is based on the approximation that the mean radiance from a layer can be given by averaging the profile variables at the top and the bottom of the layer. This is a reasonable assumption for a radiometer with spectrally averaged radiance if the atmosphere is divided up into enough layers so that the assumption of homogeneity within a layer is valid. Note that care must be taken for the uppermost layer.

For optically thick cloud at infrared wavelengths the top of atmosphere overcast cloudy radiance in discrete notation is defined as:

$$L_i^{Cld} = \tau_{i,Cld} B_i(T_{Cld}) + L_i'' + \sum_{j=1}^{J_{Cld}} L_{i,j}^u \quad (7)$$

where J_{Cld} is the layer above the cloud top and there is an interpolation of the radiance from the level below the cloud top and the level above the cloud top denoted by L_i'' to provide the additional radiance from the last full layer and the cloud top. This now gives for the top of atmosphere radiance for channel i ,

$$L_i = (1 - N) L_i^{Clr} + N L_i^{Cld} \quad (8)$$

Finally the inverse of equation 6 is used to compute the equivalent black body brightness temperature from the channel radiance L_i .

2.2. The input atmospheric profile and surface variables

The full profile vector required for RTTOV-5 is listed in Table 1. The temperature (degK), specific humidity (kg/kg) and ozone profiles (kg/kg) are supplied on j pressure levels (i.e. T_j , q_j , oz_j). There is provision for a cloud liquid water concentration profile also but this has not been implemented yet. Currently the version of RTTOV-5 in use at ECMWF uses 43 pressure levels from 0.1 to 1013 hPa defined in Table 2 together with the temperature, specific humidity and ozone profile extremes in the training dataset. The code has been generalised to use any number of levels given appropriate coefficients (see below). Surface and cloud parameters are also required by

the model which are defined in Table 1. For all channels the surface emissivity can be explicitly provided or if set to zero a default value is assumed. For microwave channels over the sea the FASTEM model (*English and Hewison, 1998*) is used in RTTOV-5 to compute the surface emissivity from the sea surface temperature and surface wind speed and the computed values are returned in the surface emissivity array. At present the cloud fraction is set to zero for the microwave channels.

The basic variable that has to be computed by the RT model is the atmospheric layer optical depth or transmittance for each channel i , and for each discrete homogeneous layer of the profile. This varies with viewing angle, pressure, temperature, and absorber concentrations and so the atmosphere has to be divided up into enough levels from the surface to the top to allow the assumption of homogeneity within each level to be valid. For the results presented here the atmosphere was divided into 43 layers defined by pressure levels from 0.1 hPa to 1013 hPa which was adequate for ATOVS. Some other fast models divide the atmosphere up into layers of equal absorber amount (e.g. OPTRAN, *McMillin et al., 1995*). Note that the vertical integration of the radiative transfer in equations 4, 5 and 7 does not have to be on the same levels as the transmittance computation described below.

2.3 Transmittance Model

(a) Diverse set of atmospheric profiles

Once the discrete profile layers have been defined the channel transmittance, $\tau_{i,j}$, from layer j to space for a range of viewing angles from nadir to beyond the edge of the scan can be computed with a line-by-line transmittance model using a diverse set of atmospheric profiles of temperature, water vapour and ozone. For the temperature and water vapour profiles 42 were taken from the TIGR profile dataset (see *Matricardi and Saunders (1999)* for more details) which together with the mean profile provided 43 profiles of temperature and specific humidity (hereafter referred to as 43WV profiles). Above 100hPa the specific humidities from a HALOE dataset (*Harries et al 1996*) were used and extrapolated to the TIGR specific humidity profiles at 300hPa where the radiosondes are believed to be more reliable. This allowed a realistic description of the variability of the specific humidity profile from the surface to 0.1hPa. This is in contrast to earlier datasets where the specific humidities were only provided to 300hPa. To enable ozone to be included in the model as a variable gas, a separate dataset of 34 profiles of ozone (with temperature and water vapour) were selected from a set of 383 profiles (mainly from NESDIS but with a few extreme Antarctic profiles included) to represent the global variability of ozone profiles.

(b) Line-by-line transmittances

The line-by-line model transmittances must cover the full spectral range of all the radiometer channels of interest and provide a sufficient resolution to represent accurately the transmittances in the channel spectral bands. The models used were GENLN2 version 4 (*Edwards 1992*) for the infrared radiances and for the microwave radiances a combination of the Liebe 1989 model (*Liebe, 1989*) for water vapour but including the 1992 update of the model oxygen absorption coefficients. Line and continuum absorption for all the gases with a significant effect on the top of the atmosphere radiance are included in these models (the gases included are listed below). The water vapour continuum model in GENLN2 is based on the formulation by *Clough et al. (1989)*. The corresponding line-by-line calculations of ozone transmittance were also made using GENLN2. Scattering by aerosols was not included in any of the calculations of infrared radiances.

To allow the fast model to provide transmittances for the Stratospheric Sounding Unit (SSU) the old fast model transmittances for the three SSU channels for the new 43 profiles on 40 levels were computed and then interpolated to the new 43 levels. These transmittances are based on the former NESDIS *tranh* model transmittances (Weinreb *et al.* 1981) derived many years ago and are in need of updating.

(c) *Computation of fast model transmittances*

Several sets of level to space transmittances were computed using the line-by-line models. The mixed gas transmittance, τ^{mix} , is the transmittance due to all the uniformly mixed gases. For this study these were assumed to be carbon dioxide, oxygen, nitrous oxide, carbon monoxide, nitrogen, methane, CFC11 and CFC12. For all these constituents fixed tropospheric concentration values for the year 2005 are assumed. Some of these gases do vary in concentration both spatially and temporally but their individual effect on the channel spectrally integrated transmittances is small enough to allow these variations to be neglected for most HIRS and AMSU radiometer channels and so they were assumed constant. Both water vapour and ozone transmittances are computed separately as variable gases. As the channel transmittances are not monochromatic it is not strictly valid to multiply the transmittances of the mixed and variable gases together to compute the total layer to space transmittance. A better approximation (McMillin *et al.*; 1995) is to multiply the mixed gas channel transmittance with the total channel transmittance divided by the transmittance of mixed gases plus other variable gas transmittance for example:

$$\tau_{i,j}^{\text{tot}} = \tau_{i,j}^{\text{mix}} \cdot \frac{\tau_{i,j}^{\text{mix+ww}}}{\tau_{i,i}^{\text{mix}}} \cdot \frac{\tau_{i,j}^{\text{mix+ww+oz}}}{\tau_{i,i}^{\text{mix+ww}}} \quad (9)$$

where the superscripts denote what selection of gases were included in the line-by-line monochromatic transmittance calculations. The fast model predicts the three terms on the right hand side of equation 9 separately. For each layer, j , the “true” radiometer channel transmittances to space are computed by integrating the line-by-line model transmittances (convolved to 0.5cm^{-1} resolution) over the channel spectral responses and then ratioing the channel averaged transmittances as in the right hand side of eq. 9. For infrared instruments these spectral responses vary for each satellite so that a new set of spectrally averaged channel transmittances (rhs of eq. 9) has to be computed for each satellite. The channel transmittances for the 43 profiles, 5 local zenith angles from 0 to 60 degrees and mixed/variable gases are used together with a set of predictors from the atmospheric profile variables to compute regression coefficients which allow layer optical depths to be calculated for mixed gases, water vapour and ozone for any given input profile. More details are given in Eyre and Woolf (1988) of the theory and approximations necessary in this approach. The regression is actually performed in terms of layer optical depth, $(d_{i,j} - d_{i,j-1})$ for mixed gases, water vapour or ozone:

$$d_{i,j} = d_{i,j-1} + Y_j \sum_{k=1}^K a_{i,j,k} X_{k,j} \quad (10)$$

where K is the number of predictors (currently 9) and their definition (i.e. X_{kj} and Y_j) are given in Tables 3 and 4 for RTTOV-5. The water vapour and ozone optical depth predictors were taken from Rayer (1995) for the infrared channels. However another set of predictors listed in Table 3 were found optimal for microwave water vapour sensitive channels.



The layer to space optical depths for mixed gases, water vapour and ozone computed from equation 10 are first converted into transmittances:

$$\tau_{i,j} = e^{(-d_{i,j})} \quad (11)$$

and then combined using equation 9 to give a total layer to space transmittance, (i.e. $\tau_{i,j}^{tot}$) which can then be used in the radiative transfer calculation defined in equations 4, 5 and 7 to compute the top of atmosphere upwelling radiance for each channel, by summing the radiance from each layer and the surface/cloud top.

3. PERFORMANCE OF THE FAST MODEL FOR TOVS AND ATOVS

3.1. Comparison with line-by-line model computed transmittances and radiances

The transmittances and radiances computed from the fast model can be compared with the corresponding “true” values from line-by-line models in several different ways. Firstly the line-by-line model transmittance profiles and top of atmosphere radiances computed from the dependent set of profiles, from which the coefficients were computed, can be compared with the fast model equivalents to determine the accuracy of the fast model itself.

For the HIRS channels (except channel 9) the dependent set of transmittances and radiances were computed using GENLN2 for the 43WV profiles and 5 viewing angles with a climatological mean value for ozone. For the ozone transmittance calculation the 34 ozone profiles from which GENLN2 transmittances were computed were the dependent set. The AMSU and MSU channel radiances were computed, as for the HIRS radiances, from the 43WV profiles using the Liebe model described above.

Secondly an independent set of profiles can be used to validate RTTOV-5 radiances with a different line-by-line model to allow spectroscopic and uncertainties from different types of profile to be included in the validation. The independent set of HIRS radiances was computed for the 528 Satellite Ozone Data Assimilation (SODA) profiles using FASCOD 3P (Clough *et al.*, 1989) as the line-by-line model. These profiles were selected from 22 radiosonde stations widely spaced over the Earth which include ozonesonde profile measurements. The distribution of the data in latitude and time of year was selected to be uniform and was designed to cover the full range of atmospheric ozone profiles. It also covers a wide range of temperature and water vapour profiles which at some levels exceed the extremes included in the 43 profile dependent set. All profiles of temperature, water vapour and ozone were interpolated on to the 43 standard pressure levels used by the fast model. The FASCOD 3P line-by-line radiances were computed from the original profile levels using the HITRAN 92 spectroscopic database (Rothman *et al.*, 1992) with a formulation for the water vapour continuum given by Clough (1995). HIRS infrared brightness temperatures for the TOVS channels on the NOAA-14 satellite were computed for different surface and viewing geometry conditions.

The analysis of the results below concentrates on the error of the fast models in terms of the bias and standard deviation of the radiance differences between the fast and line-by-line simulations. Although the radiance biases are important to be minimised they can be “corrected” before being presented to the assimilation system so that

their global bias with respect to the NWP analyses is close to zero averaged over a period of several weeks. Various radiance bias correction schemes exist for NWP radiance assimilation (e.g. Eyre 1992).

(a) Results for TOVS channels

The primary variable simulated by the model is layer optical depth using equation 10. Figure 1 shows the standard deviation of the transmittance differences for a selection of HIRS channels for RTTOV-5 for the dependent set of 43 profiles for all 5 local zenith angles from 0° to 60°. The water vapour channels are clearly more difficult to model with errors up to 2% in transmittance at 600hPa than the window (HIRS-8) and temperature sounding channels (not shown). The mean biases in the transmittances were generally less than the standard deviations (e.g. -0.6% for HIRS-12 peaking at 200hPa). The results for the ozone channel (HIRS-9) transmittances (shown in Saunders et al. 1999b) show the layer to space ozone transmittances could be computed by the fast model to an accuracy of 0.6%. The biases of the ozone transmittances were less than 0.05% at all levels.

The performance of RTTOV-5 for the HIRS and MSU channels of NOAA-14 in terms of bias and standard deviation of the difference between the fast and line-by-line computed radiances in units of equivalent black body brightness temperature for the dependent 43 profile set is given in Table 5. Radiances for all 5 local zenith angles are included in the statistics. The 43 profile set of radiances is used in the comparison for all but HIRS channel 9, which could not be included due to the assumption of a constant ozone profile for this set. Also listed are the noise equivalent temperatures ($Ne\Delta T$) for each of the channels (for a typical mean target temperature), taken from the NOAA-14 HIRS/2 pre-launch test data. The $Ne\Delta T$ values should be the target accuracy for the fast models. The radiance biases have a similar magnitude to the standard deviation and range from less than 0.01K for some channels to -0.11K for the HIRS-12 upper tropospheric water vapour channel. The biases and standard deviations for RTTOV-3 are given in Table 2 of Rizzi and Matricardi (1998) but for a different profile dataset with less extreme profiles. For the temperature sounding channels the fast model errors are less than the $Ne\Delta T$ values but for the window (7-8, 13) and water vapour (10-12) channels the fast model errors exceed the $Ne\Delta T$ values in some cases by up to 0.3K. There is obviously room for improvement for the simulation of these channels.

Figure 2 and Table 5 give the differences of the model for the HIRS channels as compared to the SODA profile radiance set for nadir views with only profiles within the 43WV profile extremes included (391) as indicated by the return flag from RTTOV-5. The model can be used for profiles beyond the extremes but more work is needed to determine how far outside the training set the model is valid so for this comparison a strict definition was used. Several conclusions can be drawn from comparing the biases and standard deviations in Table 5 for the dependent (GENLN2 based) and independent (FASCOD based) sets. Firstly for all the channels the differences for the dependent set are much less than for the independent set, for the temperature sounding channels by an order of magnitude. This shows that the differences between the two line-by-line models (GENLN2 and FASCOD) can dominate the fast model errors. For the HIRS longwave temperature sounding channels (1-3) the fast model still manages to reproduce the independent line-by-line model radiances to an accuracy less than the $Ne\Delta T$ value. Therefore any significant errors in the computed radiances for these channels are more likely to originate from the specification of the instrument spectral response than from the fast model itself. The biggest errors of the fast model in terms of both bias and standard deviation are for the HIRS water vapour channels (8, 10, 11 and 12).



The ozone channel (HIRS 9) radiance errors are significantly smaller than for the water vapour channels both in bias and standard deviation. The corresponding values for the NOAA-15 HIRS channels are similar to those for NOAA-14.

(b) Results for AMSU channels

The performance of RTTOV-5 for the AMSU channels is plotted in Figure 3 in the same format as Figure 2 but for the 43WV profile dependent set. A constant surface emissivity of 0.65 was assumed for these results, with all 5 viewing angles for each profile included. As for HIRS, all the temperature sounding channels (4-14) have fast model errors well below the $Ne\Delta T$ values for the dependent set. However for the window channels (2-3, 15-17) and water vapour channels (1,18-20) the standard deviations of the fast model exceed the $Ne\Delta T$ values in some cases. AMSU channels 19 and 20 appear to be the least accurately predicted by the fast model. The fast model biases are all within the standard deviations. The differences between line-by-line models are believed to be smaller for the microwave region than the infrared, and so the dependent set of statistics are more representative of the total radiative transfer model errors. The performance of the model on an independent set of 32 profiles taken from the TIGR set was evaluated and the biases and standard deviations between the fast and Liebe line-by-line model were less than the dependent set for all AMSU water vapour channels probably because the profiles were less extreme. For the temperature sounding channels the differences were similar.

3.2 Comparison of fast model radiances with measurements

Another way to assess the performance of the fast model is to compare the radiances computed from NWP model first guess fields with measured radiances. This has the advantage of providing an end to end evaluation of the fast model. The disadvantage is that errors in the instrument calibration, data preprocessing, finite instrument $Ne\Delta T$ and inaccurate NWP model first guess profiles all add uncertainties to the comparisons. Nevertheless these radiance differences, after bias correction, are presented to an NWP model for direct radiance assimilation and the reasons for the differences need to be understood. Table 5 lists the mean bias and standard deviation of the difference between the measured and first guess brightness temperatures for the HIRS and MSU channels averaged over a 13 day period in August/September 1998 for the latitude band 20-60°N where the NWP fields are the most accurate. The first guess radiances were computed using both RTTOV-3 and RTTOV-5 for comparison with the measurements and the standard deviation of the differences are plotted in Figure 4. The first guess comparisons are based on about 36,000 clear ocean soundings for HIRS channels 4-15 and 90,000 clear and cloudy soundings for HIRS channels 1-3 and MSU 2-4 over this 13 day period for NOAA-14. The measured TOVS radiances were generated from the NESDIS RTOVS pre-processing system which maps the MSU radiances to the HIRS field of view, applies a limb correction to nadir and classifies the data into cloudy and clear soundings. For the higher sounding channels (HIRS 1-3, 12), MSU-4 and SSU all radiances over land and sea are compared. It is instructive to compare with TOVS-1b radiances which have no pre-processing applied. For the HIRS channels the standard deviations of the model with these raw radiances is similar suggesting the NWP, instrument and radiative transfer model errors dominate the differences for this latitude band average. For AMSU-A the values were computed from the difference between measured AMSU-A 1b radiances after quality control and the model equivalents computed from RTTOV-5 for the same latitude band but for a 24 day period from 3-26 December 1998. Note that the FASTEM surface emissivities were not computed but a constant value assumed



which increases the first guess surface emissivity errors. The AMSU-A channels 5-13 were assimilated and so would be expected to have smaller first guess differences.

The standard deviation of the radiance differences (i.e. measured - computed) plotted in Figure 4 show the differences between RTTOV-3 (HARTCODE 40 levels) and RTTOV-5 (GENLN2 43 levels) with measured radiances, after quality control to help remove some of the data still contaminated by undetected clouds. The standard deviation with RTTOV-5 is slightly reduced for nearly all channels but for the upper tropospheric water vapour channel (HIRS-12) the reduction is significant (0.3K). The reduction in HIRS channel 16 is probably due to more accurate spectroscopy from GENLN2 in this spectral region (i.e. inclusion of nitrogen continuum). For MSU and SSU the differences are the same. For AMSU-A only the RTTOV-5 values were available. The surface sensing channels (AMSU-A 1-5 and 15 or 27-31 and 42 on Figure 4) all have large differences due to the errors in the first guess surface emissivity. The upper stratospheric channels (12-14 or 39-41) also have larger differences due to larger errors in the first guess temperature.

The mean biases of the radiance differences plotted in Figure 5 are reduced for some channels but increased for others with the new model. HIRS channels 1-5 all have an increased bias, especially for HIRS-4 (but the standard deviation is reduced). The biases for HIRS channels 15-17 are significantly reduced. For the other channels the biases remain the same (MSU-1 biases are a function of the surface emissivity). For AMSU-A only the surface channels have a significant bias due to the first guess emissivity assumed, the others have biases of less than 0.3K which is similar to the instrument noise.

Figure 6 shows the standard deviations of the differences between the RTTOV-5 brightness temperatures and the measurements, the SODA/Liebe radiances and the instrument noise. The HIRS and AMSU Ne Δ T values are based on pre-launch measurements for the NOAA-14 HIRS instrument and NOAA-15 AMSU instruments. From this plot the proportion of the error due to the radiative transfer model for each channel can be estimated. For the HIRS longwave temperature sounding channels (1-3) the instrument Ne Δ T dominates the measured-model differences and so they are close to the Ne Δ T values. For the other HIRS channels (except 16) the Ne Δ T values are much less than the fast RT model errors and so other factors dominate the observation minus first guess differences. The large first guess differences for the water vapour and window channels will be partly due to errors in the first guess water vapour and surface skin temperature fields and also inadequate cloud clearing in the preprocessing which adds to the "measurement noise". The HIRS shortwave channels (13-19) all have higher standard deviations than the fast model errors, when compared with measurements (note the channel 16 results are dominated by an anomalous Ne Δ T value for NOAA-14). For HIRS channels 17-19 reflected solar radiation, not included in the forward model, will contribute in addition to the other factors to the differences with the measurements. MSU-1 has a high standard deviation with measured data (8.7K) due to uncertainties in the sea surface microwave emissivity (a constant value of 0.6 was assumed for the model first guess radiances). The other MSU channels have much lower standard deviations (0.3-0.4K) comparable to the Ne Δ T values because the first guess temperature field is reasonably accurate and the fast model errors are small. This gives confidence that the fast model errors shown in Figure 3 are representative for the temperature sounding channels of AMSU. For



AMSU-A (channels 28-42 in Figure 6) the $Ne\Delta T$ values dominate the measured minus first guess differences for all but the surface and high stratospheric channels where the first guess errors become significant.

For most channels, sources of error other than the fast RT model errors dominate in practice and so the performance of the fast model presented here is adequate for radiance assimilation of most ATOVS channels. The modest improvement in the fit of the radiances to the model fields with RTTOV-5 is worthy of implementation as the fast model accuracy will become more important as the NWP model fields and basic line-by-line models become more accurate in the future. For channels where the measured minus model differences are close to the $Ne\Delta T$ value (e.g. HIRS-1-3, 16, MSU 2-4 and AMSU-A 5-12), the instrument noise is the main factor determining the observation errors. In this case the radiances from these channels could be given a greater weight in the NWP analysis if the $Ne\Delta T$ figures could be reduced through improvements in the instrument performance. The HIRS channels most influenced by the fast model errors appear to be HIRS 4, 5 and 6. For the other HIRS channels, MSU and AMSU other factors such as instrument noise, first guess errors and preprocessing of the measurements are more important.

4. SUMMARY

The RT model now in operational use at ECMWF and UKMO for radiance assimilation, RTTOV-5, uses a revised set of predictors for the water vapour layer optical depth. The set recommended by Rayer (1995) work best for the HIRS channels but an alternative set was found to give better results for the AMSU channels. The model has been enhanced to include water vapour above 300hPa and ozone as a variable gas which allows a realistic prediction of HIRS channel 9 radiances and improved prediction of the other HIRS longwave sounding channels if the ozone profile is known.

RTTOV-5 has been validated both for the computed transmittance profiles and the top of atmosphere radiances for dependent and independent profile sets and by comparisons with ATOVS measured radiances using NWP fields to provide a first guess profile. The various contributions to the observed minus first guess differences have also been analysed. For HIRS channels 1-3 (and 16 for NOAA-14), MSU channels 2-4 and AMSU-A channels 5-12 the instrument $Ne\Delta T$ values approach the measured minus first guess differences suggesting for these channels at least there is a case for an improved specification of the $Ne\Delta T$ values for NWP applications. Conversely for the tropospheric temperature, water vapour, ozone and window channels of HIRS the instrument noise is significantly less than the forward model errors for cloudfree ocean scenes but the observed minus first guess radiance field differences are much bigger than the radiative transfer errors. For HIRS channels 5, 6 and 15 (also 16 when the $Ne\Delta T$ is in specification) the forward model errors are comparable to the measured minus first guess differences and so here improvements in the RT model will clearly benefit the radiance assimilation.

The RTTOV-5 model continues to be developed within the framework of the NWP satellite application facility (SAF) co-ordinated and part-funded by EUMETSAT. In the near future it is intended to improve the simulation of the water vapour channels, add cloud liquid water as a profile variable for the microwave channels, add more instruments which can be modelled (e.g. AVHRR) and include an infrared surface emissivity model. Updated versions of the model are planned to be released once a year by the NWP SAF.



5. ACKNOWLEDGMENTS

S.English (U.K. Met. Office) for the provision of the FASTEM microwave surface emissivity model. The provision of the SODA profiles and the runs of FASCOD were carried out by F. Karcher (MétéoFrance/CNRM) as part of the European Union funded SODA project. M. Matricardi was funded by EUMETSAT through a IASI prelaunch definition studies contract.

6. REFERENCES

Andersson E., Pailleux J., Thépaut J-N, Eyre J.R., McNally A.P., Kelly G.A. and Courtier P. 1994 Use of cloud cleared radiances in three/four dimensional variational data assimilation. *Q.J.Roy. Meteorol. Soc.* **120** 627-653.

Andersson E. et al. 1998 The ECMWF implementation of three dimensional variational assimilation (3D-Var). Part III: Experimental results. *Q.J. Roy. Meteorol. Soc.* **124** 1831-1860.

Clough, S.A., Kneizys, F.X., Anderson, G.P., Shettle, E.P., Chetwynd, J.H. and Abren, L.W. 1989 FASCOD3: Spectral simulation. In *proc. of the International Radiation Symposium IRS '88 Eds J. Lenoble and J.F. Geleyn. Deepak publishing.*

Clough, S.A., Kneizys, F.X. and Davis, R.W. 1989 Line shape and the water vapour continuum. *Atmospheric Research* **23**, 229-241

Clough, S.A. 1995 The water vapor continuum and its role in remote sensing. *Optical Remote Sensing of the Atmosphere 2 OSA Tech. Dig. Ser.* 76-78

Derber J. and Wu W. 1998 The use of TOVS cloud-cleared radiances in the NCEP SSI analysis system. *Mon. Wea. Rev.* **126** 2287-2299.

Edwards, D P 1992 "GENLN2. A general Line-by-Line Atmospheric Transmittance and Radiance Model," NCAR Technical note *NCAR/TN-367+STR (National Center for Atmospheric Research, Boulder, Co., 1992).*

English S. and T.J. Hewison 1998 A fast generic millimetre wave emissivity model. *Microwave Remote Sensing of the Atmosphere and Environment Proc. SPIE* **3503** 22-30

Eyre J.R. and Woolf H.M. 1988 Transmittance of atmospheric gases in the microwave region: a fast model. *Applied Optics* **27** 3244-3249

Eyre J.R. 1991 A fast radiative transfer model for satellite sounding systems. *ECMWF Research Dept. Tech. Memo.* **176** (available from the librarian at ECMWF).

Eyre, J.R. 1992 A bias correction scheme for simulated TOVS brightness temperatures. *ECMWF Research Dept. Tech. Memo.* **186** (available from the librarian at ECMWF).

Eyre J.R., Kelly G.A., McNally A.P., Andersson E. and Persson A. 1993 Assimilation of TOVS radiance information through one-dimensional variational analysis. *Q.J.Roy. Meteorol. Soc.* **119** 1427-1463.



- Harries, J.E., Russel, J.M., Tuck, A.F., Gordley, L.L., Purcell, P., Stone, K., Bevilacqua, R.M., Gunson, M., Nedoluha, G. and Traub, W.A. 1996 "Validation of measurements of water vapour from the Halogen Occultation Experiment (HALOE)," *J. Geophys. Res.* **101**, 10205-10216
- Kelly G.A., Tomassini, M. and Matricardi, M. 1996 Meteosat cloud cleared radiances for use in three/four dimensional variational data assimilation. *Proc. of 3rd Winds Workshop, Ascona, 10-12 June 1996, pub EUMETSAT 105-116*
- Kelly G.A. 1997 Influence of observations on the operational ECMWF system. *W.M.O. Bulletin* **46** 336-341.
- Lauritson L., Nelson, G.J. and Porto, F.W. 1979 Data extraction and calibration of TIROS-N/NOAA radiometers. *NOAA Tech. Memo. NESS 107*.
- Liebe H. J. 1989 MPM- an atmospheric millimetre wave propagation model. *Intl. J. Infrared and Millimetre Waves* **10** 631-650.
- Matricardi M and Saunders R.W. 1999 A fast radiative transfer model for simulation of IASI radiances. *Applied Optics (in press)*.
- Miskolczi F., Rizzi R., Guzzi R. and Bonzagni M.M. 1988 A new high resolution atmospheric transmittance code and its application in the field of remote sensing. *Proc IRS'88 Current problems in Atmospheric Radiation, Lille 18-24 August 1988* 388-391.
- McMillin L.M., Fleming H.E. and Hill M.L. 1979 Atmospheric transmittance of an absorbing gas. 3: A computationally fast and accurate transmittance model for absorbing gases with variable mixing ratios. *Applied Optics* **18** 1600-1606
- McMillin L.M., Crone L.J. and Kleespies T.J. 1995 Atmospheric transmittance of an absorbing gas. 5. Improvements to the OPTRAN approach. *Applied Optics* **34** 8396-8399.
- Rabier F., Thépaut, J-N. and Courtier, P. 1998 Extended assimilation and forecast experiments with a four dimensional variational assimilation system. *Q.J. Roy. Meteorol. Soc.* **124**, 1861-1887.
- Rayer P.J. 1995 Fast transmittance model for satellite sounding. *Applied Optics*, **34** 7387-7394.
- Rizzi R. and Matricardi M. 1998 The use of TOVS clear radiances for NWP using an updated forward model. *Q.J. Roy. Meteorol. Soc.* **124**, 1293-1312
- Rothman L. S., Gamache R.R., Tipping R.H., Rinsland C.P., Smith M.A.H., Benner C.D., Malathy Devi V., Flaud J-M., Camy-Peyret C., Perrin A., Goldman A., Massie, S.T., Brown L.R., Toth R.A. 1992 The HITRAN molecular database: editions of 1991 and 1992. *J. Quant. Spectrosc. Radiat. Transfer* **48** 469-507.
- Saunders, R.W., Andersson, E., Kelly, G., McNally, A. and Harris, B. 1997. The direct assimilation of TOVS radiances at ECMWF. *Tech. Proc. of ITSC-IX, Igls, Feb 20-26, 1997* 417-427.
- Saunders, R.W., E. Andersson, G. Kelly, R. Munro and B. Harris 1999a Recent developments at ECMWF in the assimilation of TOVS radiances. *Tech. Proc. of ITSC-X, Boulder, Jan 27 - Feb 2, 1999*



Saunders R.W., M. Matricardi and P. Brunel 1999b An Improved Fast Radiative Transfer Model for Assimilation of Satellite Radiance Observations. *QJRM*, **125**, 1407-1425.

Smith W.L., Woolf H.M., Hayden C.M., Wark D.Q. and McMillin L.M., 1979: The TIROS-N Operational Vertical Sounder. *Bull. Am. Meteorol. Soc.*, **60**, 1177-1187.

Thépaut, J-N. and Moll, P., 1990: Variational inversion of simulated TOVS radiances using the adjoint technique. *Q.J.Roy. Meteorol. Soc.*, **116**, 1425-1448.

Weinreb, M.P., Fleming, H.E., McMillin, L.M. and Neuendorffer, A.C. 1981 Transmittances for the TIROS Operational Vertical Sounder. *NOAA Tech. Rep. NESS 85*.



Position in vector/element	Profile Array Contents	Units
1 to NLEV/1	Temperature profile	degK
1 to NLEV/2	Water vapour profile	Kg/Kg
1 to NLEV/3	Ozone profile	Kg/Kg
1 to NLEV/4	Liquid water concentration profile (not used)	
Position in vector	Surface Array Contents	Units
1	Surface 2m temperature	degK
2	Surface 2m water vapour	Kg/Kg
3	Surface pressure	hPa
4	2 m vector wind speed u	m.s ⁻¹
5	2 m vector wind speed v	m.s ⁻¹
Position in vector	Surface Skin Array Contents	Units
1	Radiative skin temperature	degK
Position in vector	Cloud Array Contents	Units
1	Cloud top pressure	hPa
2	Cloud fractional cover	0-1
Position in vector	Surface Emissivity Array Contents	Units
1 to NCHAN	Surface emissivity (if set to zero provide default value as defined in Table A2)	0-1

Table 1. Profile vectors for model. NLEV is the number of profile levels and NCHAN the number of channels. All the arrays have another dimension for profile number to allow vectorising of the code.



Pressure	Tmax (K)	Tmin (K)	Qmax (Kg/Kg)	Qmin (Kg/Kg)	Ozmax (Kg/Kg)	Ozmin Kg/Kg
0.10	305.00	180.00	0.3649E-04	0.1500E-05	0.1500E-04	0.1000E-06
0.29	305.26	192.36	0.3877E-04	0.1500E-05	0.1500E-04	0.2000E-06
0.69	320.73	187.68	0.3841E-04	0.1500E-05	0.1200E-04	0.5000E-06
1.42	322.18	178.72	0.3761E-04	0.1500E-05	0.2000E-04	0.5000E-06
2.61	317.65	178.35	0.3571E-04	0.1500E-05	0.2400E-04	0.1000E-05
4.41	298.87	178.07	0.3547E-04	0.1500E-05	0.2800E-04	0.1000E-05
6.95	292.21	176.06	0.3635E-04	0.1500E-05	0.3200E-04	0.1000E-05
10.37	272.98	171.85	0.3627E-04	0.1500E-05	0.3200E-04	0.1000E-05
14.81	268.20	172.07	0.3339E-04	0.1500E-05	0.3000E-04	0.1000E-05
20.40	262.74	167.86	0.3357E-04	0.1500E-05	0.2500E-04	0.1000E-05
27.26	260.44	167.96	0.3479E-04	0.1500E-05	0.2100E-04	0.1000E-05
35.51	259.35	168.46	0.3018E-04	0.1500E-05	0.2000E-04	0.1000E-05
45.29	258.36	169.42	0.2857E-04	0.1500E-05	0.1900E-04	0.5000E-06
56.73	258.03	171.37	0.2772E-04	0.1500E-05	0.1600E-04	0.3000E-06
69.97	257.00	173.00	0.2695E-04	0.1500E-05	0.1400E-04	0.5000E-07
85.18	256.99	170.97	0.2504E-04	0.1500E-05	0.1200E-04	0.1000E-07
102.05	255.86	168.31	0.2419E-04	0.1500E-05	0.9800E-05	0.1000E-07
122.04	254.64	174.07	0.2979E-04	0.1500E-05	0.6500E-05	0.2000E-08
143.84	253.25	174.86	0.7176E-04	0.1500E-05	0.5100E-05	0.5000E-09
167.95	253.45	177.44	0.1369E-02	0.1500E-05	0.3800E-05	0.5000E-09
194.36	254.67	181.37	0.2322E-02	0.1500E-05	0.2700E-05	0.5000E-09
222.94	256.64	183.70	0.3696E-02	0.1500E-05	0.2000E-05	0.1000E-09
253.71	259.33	185.17	0.6370E-02	0.1500E-05	0.1500E-05	0.1000E-09
286.60	262.42	186.20	0.9307E-02	0.1500E-05	0.1200E-05	0.5000E-09
321.50	267.28	189.51	0.1401E-01	0.1500E-05	0.1000E-05	0.5000E-09
358.28	273.22	193.54	0.2119E-01	0.1500E-05	0.6700E-06	0.5000E-09
396.81	278.56	194.82	0.3019E-01	0.1500E-05	0.6000E-06	0.5000E-09
436.95	283.83	198.64	0.4168E-01	0.1500E-05	0.5700E-06	0.5000E-09
478.54	288.33	202.30	0.5419E-01	0.2434E-05	0.5400E-06	0.5000E-09
521.46	291.87	205.58	0.6461E-01	0.5635E-05	0.5200E-06	0.5000E-09
565.54	295.66	208.70	0.7458E-01	0.1301E-04	0.4900E-06	0.5000E-09
610.60	298.33	211.45	0.8783E-01	0.1617E-04	0.4700E-06	0.5000E-09
656.43	302.68	214.17	0.1033	0.1780E-04	0.4500E-06	0.5000E-09
702.73	306.20	217.12	0.1175	0.2133E-04	0.4200E-06	0.5000E-09
749.12	309.69	219.03	0.1323	0.4537E-04	0.3700E-06	0.5000E-09
795.09	313.13	220.42	0.1479	0.6679E-04	0.3500E-06	0.5000E-09
839.95	316.39	221.14	0.1663	0.8028E-04	0.3400E-06	0.5000E-09
882.80	318.48	219.40	0.1781	0.8350E-04	0.3400E-06	0.5000E-09
922.46	320.14	217.19	0.2002	0.8209E-04	0.3400E-06	0.5000E-09
957.44	322.46	209.05	0.2247	0.8209E-04	0.3200E-06	0.5000E-09
985.88	324.17	172.17	0.2324	0.8209E-04	0.3100E-06	0.5000E-09
1005.43	325.33	150.00	0.2350	0.8209E-04	0.2600E-06	0.5000E-09
1013.25	350.79	150.00	0.2365	0.8209E-04	0.1900E-06	0.5000E-09

Table 2. Pressure levels and max/min profiles adopted for RTTOV-5

Predictors	uniformly mixed gases	HIRS water vapour/ ozone	AMSU water vapour/ozone
X_{1j}	$\delta T_j \sec \theta$	δT_j	δT_j
X_{2j}	$\overline{\delta T_j^2} \sec \theta$	$\overline{p \delta T_j}$	$\overline{p \delta T_j}$
X_{3j}	$\overline{\delta T_j} \sec \theta$	δq_j	δq_j
X_{4j}	$\overline{p \delta T_j} \sec \theta$	$\overline{p \delta q_j}$	$\overline{p \delta q_j}$
X_{5j}	$(\sec \theta - 1)$	$\delta T_j (\sec \theta u_j)^{1/2}$	$\delta T_j (u_j)^{1/2}$
X_{6j}	$(\sec \theta - 1)^2$	$\delta T_j^2 (\sec \theta u_j)^{1/2}$	$\delta T_j^2 (u_j)^{1/2}$
X_{7j}	$\overline{\delta T_j} (\sec \theta - 1)$	$\delta q_j (\sec \theta u_j)^{1/2}$	$\delta q_j (u_j)^{1/2}$
X_{8j}	$\overline{p \delta T_j} (\sec \theta - 1)$	$(\sec \theta - 1) (\sec \theta u_j)^{1/2}$	0
X_{9j}	$\overline{\delta T_j} (\sec \theta - 1)$	$(\sec \theta - 1)^2 (\sec \theta u_j)^{1/2}$	0
Y_j	1	$(\sec \theta u_j)^{1/2}$	$(\sec \theta u_j)^{1/2}$

Table 3: Model predictors for mixed gases, and old and new versions for water vapour/ozone. The profile variables are defined in Table 4 below.

$$\begin{aligned} \overline{\delta T_j} &= \frac{1}{p_j} \sum_{\ell=1}^j \delta T_\ell (p_\ell - p_{\ell-1}) & u_j &= \frac{1}{2} (q_j + q_{j-1}) (p_j - p_{j-1}) \\ \overline{p \delta T_j} &= \frac{2}{p_j^2} \sum_{\ell=1}^j p_\ell \delta T_\ell (p_\ell - p_{\ell-1}) & \overline{p \delta q_j} &= \frac{2}{p_j^2} \sum_{\ell=1}^j p_\ell \delta q_\ell (p_\ell - p_{\ell-1}) \\ \delta T_j &= \frac{1}{2} (T_j - T_j^{ref} + T_{j-1} - T_{j-1}^{ref}) & \delta q_j &= \frac{1}{2} (q_j - q_j^{ref} + q_{j-1} - q_{j-1}^{ref}) \end{aligned}$$

T_j and q_j are the temperature and specific humidity or ozone volume mixing ratio profiles. T_j^{ref} and q_j^{ref} are corresponding reference profiles (the mean of a set of global water vapour and ozone profiles has been used).

Table 4: Definition of profile variables used in predictors defined in Table 3.



Channel number/ NOAA-14 Central freq (cm ⁻¹)	NeΔT ¹ degK	Line-by-line – fast model Dependent 43 profile set		FASCOD - fast model SODA profile set		Measured - fast model Over 15 days 20-60°N	
		Bias degK	Sdev degK	Bias degK	Sdev degK	Bias degK	Sdev degK
1/669	1.86	0.01	0.04	-0.44	0.32	-1.26	1.54
2/679	0.44	0.00	0.02	-0.25	0.21	-0.54	0.44
3/690	0.30	0.00	0.01	-0.04	0.24	0.22	0.43
4/704	0.12	0.01	0.04	0.66	0.32	2.90	0.32
5/714	0.09	0.01	0.05	0.79	0.29	2.50	0.34
6/733	0.06	0.00	0.05	0.88	0.41	0.50	0.58
7/750	0.04	0.00	0.08	0.71	0.48	1.01	1.06
8/899	0.01	0.00	0.06	0.60	0.60	-0.35	1.99
9/1028	0.03	-	-	-0.04	0.56	-	-
10/796	0.07	-0.01	0.13	0.52	0.58	-0.71	1.63
11/1361	0.11	0.00	0.41	-0.76	0.82	0.89	2.08
12/1481	0.30	-0.11	0.59	-0.39	0.79	-1.21	2.83
13/2191	0.02	0.00	0.03	0.54	0.22	-2.72	1.08
14/2207	0.06	0.00	0.02	0.17	0.16	-1.67	0.67
15/2236	0.06	0.01	0.03	0.34	0.19	-4.32	0.49
16/2268	1.40	0.01	0.05	0.68	0.64	0.20	1.27
17/2420	0.08	0.00	0.01	0.43	0.15	-0.02	2.36
18/2512	0.01	0.00	0.00	-0.01	0.08	1.24	4.46
19/2648	0.01	-0.01	0.06	0.08	0.16	2.58	6.27
21/1.68	0.3	0.08	0.30	-	-	-	8.67
22/1.79	0.3	0.00	0.01	-	-	-0.66	0.45
23/1.83	0.3	0.00	0.00	-	-	-0.78	0.25
24/1.93	0.3	-0.01	0.01	-	-	0.41	0.53

Table 5. Biases and standard deviations of difference between line-by-line and fast model computed NOAA-14 HIRS (1-19) and MSU (21-24) brightness temperatures for a dependent set of 43 diverse profiles for the new predictors listed in Table 2 and an independent set of SODA profiles. Also listed are the standard deviation of NOAA-14 measured minus computed brightness temperatures using the ECMWF first guess fields averaged over 2 weeks in the latitude band from 20-60°N in August/September 1998 for both the old and new model. There are no first guess ozone fields at present so HIRS channel 9 is not included in the comparison with measurements

¹The HIRS values quoted are for a typical target temperature for each channel inferred from pre-launch measurements for NOAA-14. The MSU values are from the instrument specification.

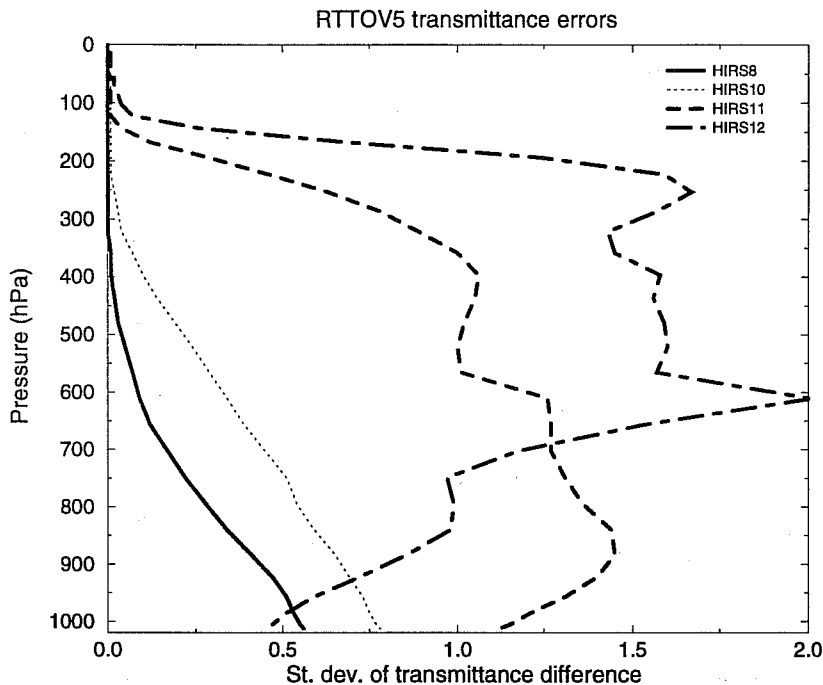


Fig. 1 Standard deviation of difference between RTTOV-5 and GENLN2 HIRS channel 8, 10, 11 and 12 layer to top of atmosphere transmittances for NOAA-14 for 43 diverse water vapour profiles and 5 viewing angles.

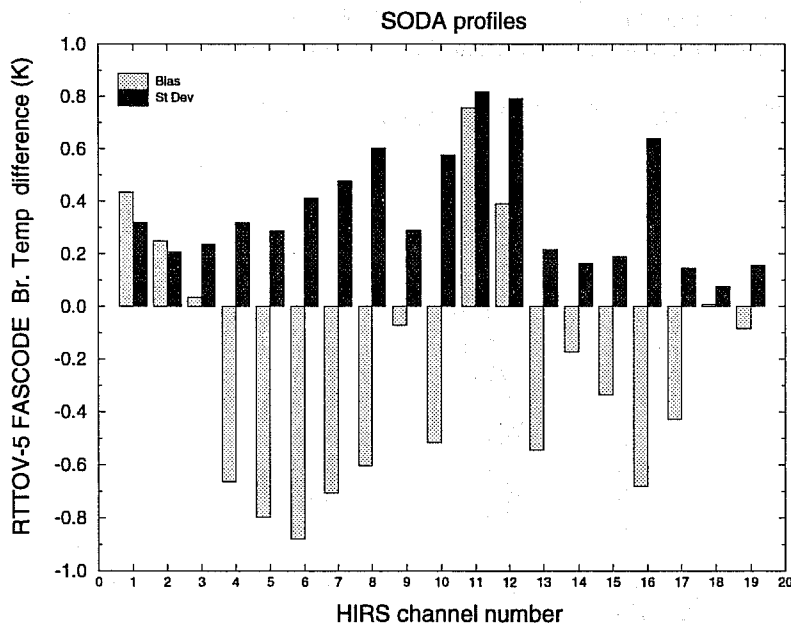


Fig. 2 Mean bias (grey) and standard deviation (black) of the difference between RTTOV-5 and FASCODE line-by-line computed NOAA-14 HIRS brightness temperatures for 391 diverse SODA profiles. Only those profiles within the dependent set extremes are included.

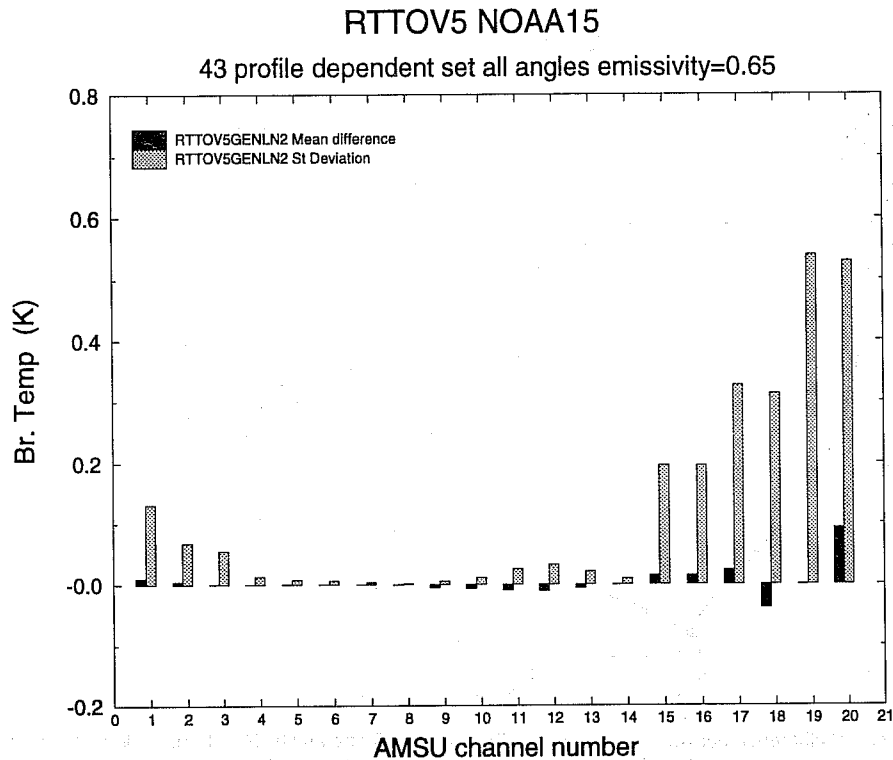


Fig. 3 Mean bias (black) and standard deviation (grey) of the difference between RTTOV-5 and the Liebe line-by-line computed AMSU brightness temperatures for the dependent 43 diverse water vapour profile set. Note some of the values are so close to zero it is difficult to see them on the plot.

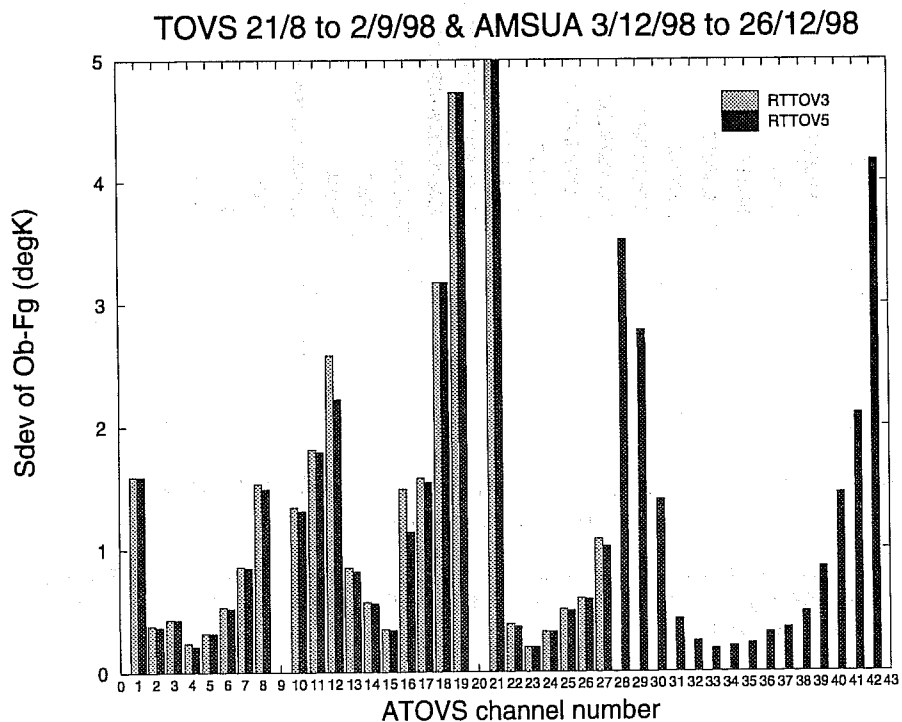


Fig. 4 Standard deviation of observed minus first guess HIRS (1-20), MSU (21-24) and SSU (25-27) brightness temperatures computed with RTTOV-5 (grey) and RTTOV-3 (black) using ECMWF first guess fields for the latitude band 20-60N averaged over the period from 21 August to 2 September 1998. Also plotted are the equivalent values for AMSU-A (28-42) over the period 3 to 26 December 1998 but only for RTTOV-5.

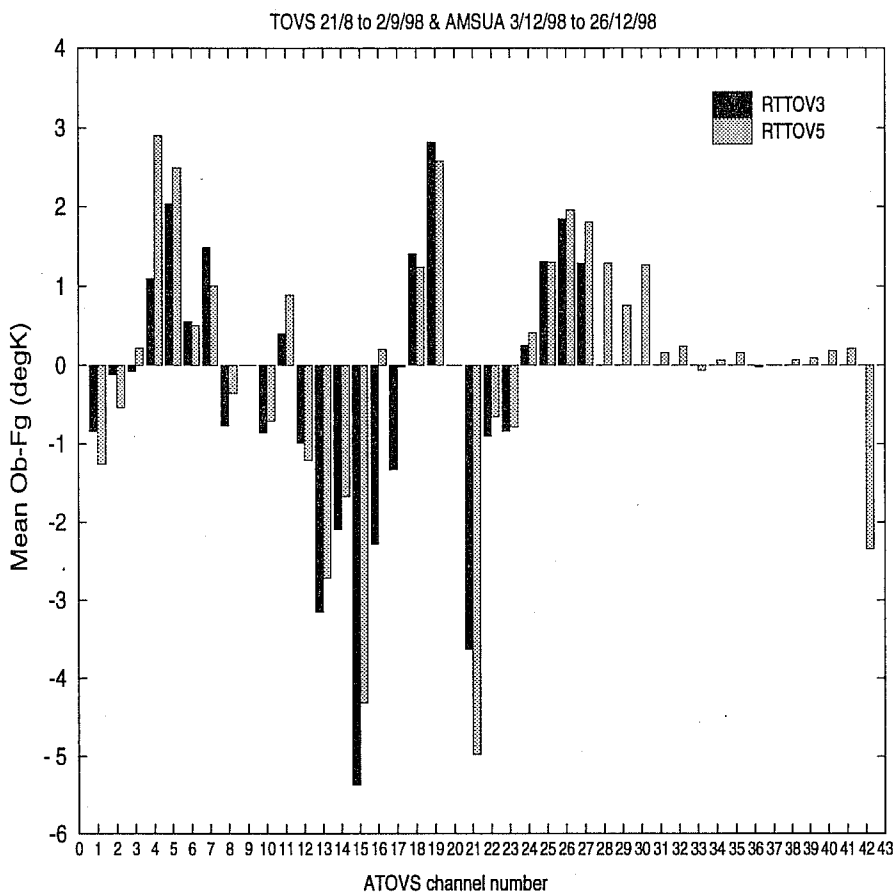


Fig. 5 As for Figure 4 but for the mean observed minus first guess brightness temperature bias.

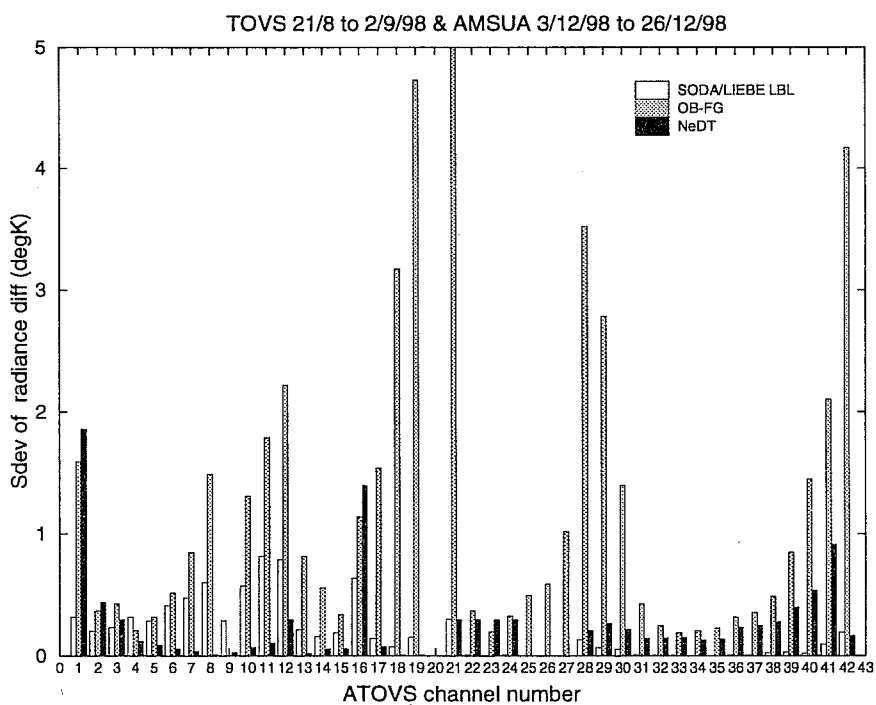


Fig. 6 As for Figure 4 but with the the instrument radiometric noise values (black) and line-by-line model (GENLN2 for infrared and Liebe for microwave channels) differences (white) also plotted.





ANNEX- 1 RTTOV-5 - TECHNICAL DESCRIPTION

1. GENERAL REMARKS

The purpose of this annex is to document the user interface to RTTOV-5. The main features of RTTOV-5 are described below in bullet form:

- It is based on the original TOVS fast radiative transfer (RT) model RTTOV-3 (Eyre, 1991), using the same basic structure of the code as far as possible and coding rules for TL, AD and K routines.
- It supports many satellite IR and microwave passive radiance observations (e.g. TOVS, ATOVS, VTPR, SSM/I, METEOSAT imager, etc.) with the same code but using different RT coefficient files as input. A single documented ASCII RT coefficient file is used as input for each satellite series type. This facilitates export of the code and makes it clear what values are used. The code does however accept a binary input for operational purposes where I/O is an important consideration.
- It allows a different surface emissivity to be input for each radiometer channel and if the input is set to zero sensible default values are assumed in the model and returned in the output. For microwave channels over the ocean the FASTEM model (English and Hewison, 1998) is used if the input is zero.
- It has a more flexible user interface to permit input of new variables (e.g. profiles of ozone and liquid water, and more surface and cloud parameters) and to allow easy future extension to other input variables (e.g. profiles of ice water, precipitation, aerosol, etc.). This involves a compromise between allowing initially for all input variables which might be required, and keeping the number of input variables reasonably small (since this affects the memory requirements, particularly for the associated adjoint and K-matrix calculations).
- A check is applied on the input profile variables to make sure they are within the limits of the regression used to compute the coefficients. If they are outside the limits but still physically reasonable a calculation will still be performed but a flag is returned in the range (10-19). If the profile is not physically reasonable RTTOV will return with an error flag >20 set.
- It outputs intermediate products of the RT calculations in addition to simulated radiances and brightness temperatures (e.g. surface to space transmittances, transmittances profiles etc).

2 DOCUMENTATION OF RTTOV-5 CODE STRUCTURE

The code requires a call to two subroutines *RTTVI* to set up the necessary arrays for the satellite series required (e.g. NOAA, METEOSAT, DMSP, GOES GMS) and the satellite ids for each series (e.g NOAA-14,15, METEOSAT,7 MSG-1, F13/F14 etc). The *cparam.h* include file defines the array sizes for running RTTOV-5. It is recommended the user modifies this file to set the array size for his particular application.



The variables in the file are defined in Table A.1. If the `rt_coefficient` file supplied is used then only those variables in *italics* should be modified. **JPNSAT** refers to the maximum number of satellites of all series to be used at any one time, **JPPF** to the maximum number of profiles to be processed in any one call to RTTOV and **JPCHUS** to the maximum number of channels required to be simulated by RTTOV.

PARAMETER (JPTOVS=15)	! MAX NO. OF TOVS/ATOVS SATS IN COEF FILE
PARAMETER (JPDMS= 7)	! MAX NO. OF DMSP SATS IN COEF FILE
PARAMETER (JPMET = 4)	! MAX NO. OF METEOSAT SATS IN COEF FILE
PARAMETER (JPGOES= 2)	! MAX NO. OF GOES SATS IN COEF FILE
PARAMETER (JPGMS = 1)	! MAX NO. OF GMS SATS IN COEF FILE
<i>PARAMETER (JPNSAT=12)</i>	<i>! MAX NO. OF SATELLITES TO BE USED</i>
PARAMETER (JPLEV=43)	! NO. OF PRESSURE LEVELS IN PROFILE
PARAMETER (JPNAV=4)	! NO. OF PROFILE VARIABLES IN PROFILE
PARAMETER (JPNSAV=5)	! NO. OF SURFACE AIR VARIABLES
PARAMETER (JPNSSV=1)	! NO. OF SKIN VARIABLES
PARAMETER (JPNCV=2)	! NO. OF CLOUD VARIABLES
<i>PARAMETER (JPPF=1)</i>	<i>! MAX NO. PROFILES FOR EACH RTTOV CALL</i>
PARAMETER (JPCH=47)	! MAX. NO. OF (A)TOVS CHANNELS IN PARAM FILE
PARAMETER (JPHIR=20)	! MAX. NO. OF HIRS CHANNELS IN PARAM FILE
PARAMETER (JPMSU=4)	! MAX. NO. OF MSU CHANNELS IN PARAM FILE
PARAMETER (JPAMSU=20)	! MAX. NO. OF AMSU CHANNELS IN PARAM FILE
PARAMETER (JPSSU=3)	! MAX. NO. OF SSU CHANNELS IN PARAM FILE
PARAMETER (JPVTPR=16)	! MAX NO. OF VTPR CHANNELS IN PARAM FILE
<i>PARAMETER (JPCHUS=39)</i>	<i>! MAX. NO. OF CHANNELS REQ'D FOR COMPUTATION</i>
PARAMETER (JPCHPF=JPPF*JPCHUS)	! MAX NO. OF PROFS * CHANS REQUIRED
PARAMETER (JPCOFM=10)	! MIXED GAS COEFFS (MAX)
PARAMETER (JPCOFW=10)	! WATER VAPOUR COEFFS (MAX)
PARAMETER (JPCOFO=10)	! OZONE COEFFS (MAX)
PARAMETER (JPST=10)	! MAX NO. OF SURFACE TYPES

† (set to 1 for scalar machine, and to ~50 for a vector machine for optimal performance)

Table A1. RTTOV-5 include file `cparam.h`



There are 2 subroutine calls required to run RTTOV-5: **RTTVI** and **RTTOV**. The former set up the arrays and loads in all the constants from the `rt_coefficient` file(s) and is only called once, the latter actually performs the RT calculation for the specified satellite ids and channel numbers given valid profile arrays. The subroutine calling structure for **RTTVI** and **RTTOV** is shown in Figures A1 and A2. For users who require the tangent-linear, adjoint or K routines of RTTOV-5 the calls are **RTTOVTL**, **RTTOVAD** and **RTTOVK** respectively with the same subroutines called inside with the endings TL, AD, K. The details of the calling interfaces are given in section 3.

3 DOCUMENTATION OF RTTOV-5 INTERFACES

3.1 RTTVI Interface

```
CALL RTTVI (IERR, KPPF, KPNSAT, KPLEV, KPCH, KPCHUS, KPNAV, KPNSAV,
           KPNSV, KPNCV, NSERIES, NSATID, NSUBTYPE,
           KSERIES, KSATID, KSUBTYPE, MAXSERIES, MAXSATID,
           MAXSUBTYPE, UP, UTMN, UTMX, UQMN, UQMX, UOMN, UOMX, IVCH)
```

RTTVI is called only once for more than one satellite series; `tovcf.F`, `eumcf.F` are called from RTTVI as required.

Arguments:

Input:

NSERIES	- NUMBER OF SATELLITE SERIES REQUESTED
NSATID (MAXSERIES)	- NUMBER OF SATELLITE ID'S FOR EACH SERIES
NSUBTYPE (MAXSERIES)	- NUMBER OF SUBTYPES FOR EACH SERIES (set to 1)
KSERIES (MAXSERIES)	- LIST OF REQUESTED SERIES
KSATID (MAXSERIES, MAXSATID)	- LIST OF REQUESTED SATID'S FOR EACH SERIES
KSUBTYPE (MAXSERIES, MAXSUBTYPE)	- LIST OF REQUIRED SUBTYPES FOR EACH SERIES
MAXSERIES	- MAXIMUM NUMBER OF SERIES
MAXSATID	- MAXIMUM NUMBER OF SATELLITES PER SERIES
MAXSUBTYPE	- MAXIMUM NUMBER OF SUBTYPES FOR EACH SERIES

Output:

IERR	- ERROR FLAG, RETURNS IERR /= 0 IF ERROR
KPPF	- MAX NUMBER PROFILES PROCESSED IN PARALLEL
KPNSAT	- MAX NUMBER OF SATELLITES
KPLEV	- NUMBER OF RT LEVELS
KPCH	- MAX NUMBER OF CHANNELS
KPCHUS	- MAX NUMBER OF CHANNELS USED
KPNAV	- MAX NO OF PROFILE VARIABLES
KPNSAV	- MAX NO OF SURFACE VARIABLES
KPNSV	- MAX NO OF SKIN VARIABLES
KPNCV	- MAX NO OF CLOUD VARIABLES
PRESLEV	- KPLEV PRESSURE LEVELS FOR RT CALCULATIONS
OTMIN	- MIN TEMP PROFILE ARRAY
OTMAX	- MAX TEMP PROFILE ARRAY
OQMIN	- MIN SPECIFIC HUMIDITY PROFILE ARRAY
OQMAX	- MAX SPECIFIC HUMIDITY PROFILE ARRAY
OOZMIN	- MIN OZONE PROFILE ARRAY
OOZMAX	- MAX OZONE PROFILE ARRAY
IVCH (KPCH, KPNSAT)	- ARRAY PER SATELLITE OF VALID CHANNEL NUMBERS



Notes

Series numbers have been arbitrarily assigned as:

NOAA = 1 DMSP = 2 METEOSAT = 3 GOES = 4 GMS = 5

Satellite identifiers are:

NOAA-2 = 1 METEOSAT-5 = 5
NOAA-3 = 2 etc
NOAA-4 = 3 MSG-1 = 8
NOAA-5 = 4
TIROS-N = 5
NOAA-6 = 6
 etc
NOAA-14 = 14
NOAA-15 = 15

Satellite instrument sub-types are set to 1 at present as the parameter is not used:

(A) TOVS= 1 MVIRI=1 SEVIRI=1 etc

4. RTTOV INTERFACE: GENERAL SPECIFICATION

CALL RTTOV(KNPF, KLENPF, KNAV, KNSAV, KNSSV, KNCV, PPRES, PANGL, PANGA, PANGS, PANGSA, PGRODY, KSURF, KSAT, KNCHPF, KCHAN, KPROF, PAV, PSAV, PSSV, PCV, PEMIS, IFAIL, PRAD, PTB, PRDOV, PRDO, PTAU, PTAUSF)

The terms "constant" and "variable" are employed here in the sense used in variational analysis, i.e. an input variable is a parameter with respect to which a gradient will be calculated in the associated tangent linear (TL) and adjoint (AD) routines.

Input constants

KNPF	number of profiles (no restriction affects memory requirements)
KLENPF	length of atmospheric profile vectors
KNAV	number of atmospheric profile variables
KNSAV	number of surface air variables
KNSSV	number of surface skin variables
KNCV	number of cloud variables
PPRES(KLENPF)	pressure levels (hPa) of atmospheric profile vectors
PANGL(KNPF)	satellite local zenith angle (deg) (in 1B dataset)
PANGA(KNPF)	satellite local azimuth angle (deg) (in 1B dataset)
PANGS(KNPF)	solar zenith angle at surface (deg) (in 1B dataset)
PANGSA(KNPF)	relative satellite solar azimuth angle.
PGRODY(6)	grody type microwave emissivity coeffs
KSURF(KNPF)	surface type index (0=land, 1=sea)
KSAT	satellite index (see RTTVI)
KNCHPF	number of output radiances (= channels used * profiles)
KCHAN(KNCHPF)	channel indices (for output vectors)
KPROF(KNCHPF)	profile indices (for output vectors)



Input variables

PAV (KLENPF, KNAV, KNPF) atmospheric profile variables
 PSAV (KNSAV, KNPF) surface air variables
 PSSV (KNSSV, KNPF) surface skin variables
 PCV (KNCV, KNPF) cloud variables

Input/output variables

PEMIS (KNCHPF, KNPF) surface emissivity for each channel. If set to zero on input for microwave channels the FASTEM model is used (over sea) and the computed values returned as output (see table A2).

Output constants

IFAIL return flag (0=OK, 10-19=outside profile limits, >20=unphysical profile) See Table A3.

Output variables

PRAD (KNCHPF) radiances (mW/cm-1/ster/sq.m)
 PTB (KNCHPF) brightness temperatures (degK)
 PRDOV (KNCHPF, KLENPF) overcast radiance at each level in mW/m²/sr/cm⁻¹
 PRDO (KNCHPF) overcast radiance at given cloud top in W/m²/sr/cm⁻¹
 PTAU (KNCHPF, KLENPF) transmittance from each standard pressure level
 PTAUSF (KNCHPF) transmittance from surface

Input ϵ	Forward Output ϵ	Tangent Linear Output $\partial\epsilon$
INFRARED		
0	1.	$\partial\epsilon$ about 1
Non-zero	as input	$\partial\epsilon$ about ϵ
MICROWAVE		
0	Land/sea-ice=0.9/sea= ϵ_{FASTEM}	Land/sea-ice $\partial\epsilon$ about 0.9 / sea $\partial\epsilon$ computed from $\partial u, \partial v, \partial \text{sst}$ about ϵ_{FASTEM}
Non-zero	as input	$\partial\epsilon$ about ϵ

Table A2. Output values of ϵ and $\partial\epsilon$ arrays for infrared and microwave channels for forward and gradient routines



IFAIL value	Meaning
0	Profile OK
11	Temp profile outside limits
12	Water vapour profile outside limits
13	Ozone profile outside limits
14	Surface temp outside limits
15	Surface water vapour outside limits
16	Surface wind speed outside limits
20	Input pressure levels do not match coef file
21	Temperature profile unphysical
22	Water vapour profile unphysical
23	Ozone profile unphysical
24	Surface temperature unphysical
25	Surface water vapour unphysical
26	Surface wind unphysical
27	Surface pressure unphysical

Table A3. Values for IFAIL flag from RTTOV

5. SITE SPECIFIC IMPLEMENTATIONS OF RTTOV-5

5.1 ECMWF implementation (from CY19R2)

Input constants

KNSAT	12
KNPF	65
KLENPF	43: number of ECMWF pressure levels
KNCHPF	47*65 for (ATOVS)
KCHAN (KNCHPF)	1-20 = HIRS 1-20; 21-24 = MSU; 25-27 = SSU; 28-42 = AMSU-A; 43-47 = AMSU-B (for NOAA-2-5 1-16 = VTPR sets 1+3)
	1-2=Meteosat WV,IR
	1-8=MSG IR channels
KPROF (KNCHPF)	Profile number (1-65)

5.2 UKMO implementation (from VAR)

Input constants

KNSAT	5
KNPF	1
KLENPF	40: number of NESDIS pressure levels
KNCHPF	47: for (ATOVS)
KCHAN (KNCHPF)	1-20 = HIRS 1-20; 21-24 = MSU; 25-27 = SSU; 28-42 = AMSU-A; 43-47 = AMSU-B
KPROF (KNCHPF)	Profile number always 1

Figure A1. Subroutine tree for RTTOV-5 setup call

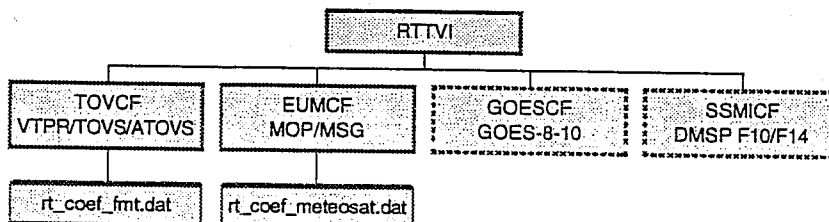


Figure A2. Subroutine tree for RTTOV-5 main call

